Korean J. Chem. Eng., 33(2), 500-506 (2016)
DOI: 10.1007/s11814-015-0189-5

pISSN: 0256-1115
eISSN: 1975-7220

CO hydrogenation to higher alcohols over Ni- and Mo-modified Cu/CeO_2 catalyst

Jun Chen, Wei Li†, and Rongchun Shen

State Key Laboratory of Chemical Engineering, East China University of Science and Technology, Shanghai 200237, China
(*Received 15 June 2015 • accepted 28 August 2015*)

Abstract−Ni-Mo promoted Cu/CeO_2 catalyst was synthesized by co-precipitation method using 28%wt $NH_3 \cdot H_2O$ as the precipitant. The catalysts were characterized by BET, XRD, TPR and XPS. The results showed that Ni and Mo could promote the reducibility of Cu, and the interaction between Ni and Mo may be needed for catalytic activity and higher alcohols synthesis. Therefore, $CuNiMo/CeO_2$ catalyst showed a higher activity for higher alcohols synthesis than Cu/CeO_2. In the meantime, the effect of pyrogallol used in preparing the $CuNiMo/CeO_2$ catalyst was investigated. Pyrogallol had a significant influence on lowering the methanol selectivity and improving the C^{2+}-OH selectivity. The methanol selectivity decreased from 52.99% to 44.81% and S_{C2+OH}/S_{MeOH} (MeOH denoted as methanol) ratio increased from 0.27 to 0.35. The XPS results gave evidence that pyrogallol can form complexes with Cu^+ on the CeO_2 support, which causes methanol decrease. In addition, pyrogallol could serve as a "temperature addictive agent" to save power.

Keywords: Co-precipitation, $NH_3 \cdot H_2O$, Higher Alcohol, Pyrogallol, Temperature Addictive Agent

INTRODUCTION

The synthesis of higher alcohols from syngas has attracted wide attention because of the depletion of fossil fuel resources and the prospect of limited oil supplies. Higher alcohols can be used as fuels, chemicals or chemical intermediates [1-3]. It has been proven that higher alcohols can be added to gasoline to increase octane rating and reduce emissions of NO_x, CO_2, and unburned hydrocarbons [4,5]. As for syngas, it can be derived from biomass, coal and natural gas [6], which are so abundant that it makes the study promising.

Typical catalysts were investigated for the hydrogenation of CO to higher alcohols, including Mo-based catalysts, Rh-based catalysts, Fischer-Tropsch synthesis catalysts and modified methanol catalysts, respectively. Mo-based catalysts are sulfur tolerant [7] and favor the formation of linear alcohols, with a high relative selectivity to ethanol; however, their commercialization is limited by high pressures and temperatures. Rh-based catalysts afford highest ethanol, but Rh metal is very expensive [8]. Modified Fischer-Tropsch synthesis catalysts give mainly C_1-C_6 linear primary alcohols as well as a large amount of hydrocarbons. Modified methanol catalysts mainly produce a mixture of methanol and isobutanol, and the higher alcohol selectivity is low [9].

Many works have been done to improve the selectivity of higher alcohol in modified methanol catalysts. For example, Beiramar et al. [10] investigated the effects of metal promotion on the performance of CuZnAl catalysts for alcohol synthesis; Xu et al. reported that the use of supercritical hexanes as a reaction medium provides opportunities to enhance the performance of higher alcohol synthesis [11]. However, compared with modified methanol catalysts, modified $Cu\text{-}CeO_2$ catalysts may be a better choice for higher alcohol synthesis. Ce is the most abundant of the rare earth elements. Cerium dioxide is widely used as a support for many oxidation catalysts because of its low temperature reducibility, oxygen storage and release properties. Xu et al. reported that CeO_x acts as structural promoter to increase the dispersion of Cu and the density of basic sites over $K\text{-}CuMgCeO_x$ catalyst, which is needed for alcohol chain growth reactions. Meanwhile, they found that the presence of Ce oxide species favored the formation of small Cu metal crystallites on MgO support, as well as decreased reduction temperature of CuO [12,13]. Kim et al. also investigated that the support for higher alcohol synthesis was neutral or basic; otherwise, could be made neutral or basic by adding alkaline promoters [14]. Liu et al. [15] found the STY (space time yield) of higher alcohol formed over Cu/CeO_2 was much larger than that over Cu/ZnO. Furthermore, when modified with Ni and Cs, Cu/CeO_2 catalyst achieved a higher activity and a higher selectivity for the synthesis of higher alcohol.

In addition, it was found that Ni was the best F-T element for increasing the selectivity of higher alcohols over Mo-based catalysts [16], and the Ni-Mo synergistic effect was essential for the activation of CO [17]. Further, Feng et al. found that the CO conversion was increased and the methanol selectivity was significantly decreased over Cu-Co-based catalysts supported on MWNT-silica gels when pyrogallol was used in preparing the catalyst [18]. However, there have been few investigations about Ni and Mo modified Cu-based catalyst for higher alcohols synthesis, as well as the effect of pyrogallol in preparing the Cu-based catalyst. So in this study, the Ni- and Mo-modified Cu/CeO_2 catalyst and the effect of pyrogallol on alcohol selectivity was investigated.

EXPERIMENTAL

1. Preparation of Catalysts

Cu/CeO_2 was prepared by a coprecipitation method using $NH_3 \cdot$

†To whom correspondence should be addressed.
E-mail: liwei@ecust.cn

H_2O as a precipitant. In a typical process, $Ce(NO_3)_3{\cdot}6H_2O$ and $Cu(NO_3)_2{\cdot}3H_2O$ at a Ce/Cu molar ratio of 4 : 1 were dissolved in deionized water. A portion of 28 wt% $NH_3{\cdot}H_2O$ was added dropwise to the aqueous solution of mixed metallic nitrates with strong stirring at room temperature till pH=13. Then the slurry was boiled up for 6 h with stirring till pH=5.5. Distillate water was added to the beaker to keep the liquid level during the boiling process. After the precipitation step, the precipitate was then filtered off, washed and dried at 383 K for 12 h. Finally, the catalyst was calcined at 450 °C for 3 h at a heating rate of 3 °C/min.

$CuNi/CeO_2$, $CuMo/CeO_2$ and $CuNiMo/CeO_2$ catalysts were prepared by the same method as Cu/CeO_2 catalyst. For $CuNi/CeO_2$ catalyst, $Ce(NO_3)_3{\cdot}6H_2O$, $Cu(NO_3)_2{\cdot}3H_2O$ and $Ni(NO_3)_2{\cdot}6H_2O$ at a Ce/Cu/Ni molar ratio of 4 : 1 : 0.3 were dissolved in deionized water. For $CuMo/CeO_2$ catalyst, $Ce(NO_3)_3{\cdot}6H_2O$, $Cu(NO_3)_2{\cdot}3H_2O$ and $(NH_4)_6Mo_7O_2{\cdot}6H_2O$ at a molar ratio of Ce/Cu/Mo=4 : 1 : 0.1 were dissolved in deionized water. For $CuNiMo/CeO_2$ catalyst, $Ce(NO_3)_3{\cdot}6H_2O$, $Cu(NO_3)_2{\cdot}3H_2O$, $Ni(NO_3)_2{\cdot}6H_2O$ and $(NH_4)_6Mo_7O_2{\cdot}6H_2O$ at a molar ratio of Ce/Cu/Ni/Mo=4 : 1 : 0.3 : 0.1 were dissolved in deionized water.

$CuNiMoP/CeO_2$ (cop) catalyst (pyrogallol was donated as P) was prepared by the same method as Cu/CeO_2, with a constant Ce/Cu/Ni/Mo/P molar ratio of 4/1/0.3/0.1/0.4.

$CuNiMoP/CeO_2$ (imp) catalyst was prepared by impregnating $CuNiMo/CeO_2$ in a pyrogallol solution, with the same Ce/Cu/Ni/Mo/P molar ratio as $CuNiMoP/CeO_2$ (cop).

2. Catalyst Evaluation

Activity tests of the catalysts for conversion of syngas to higher alcohol were carried out in a fixed-bed continuous-flow reactor-GC combination system. One milliliter of catalyst (40-80 mesh) was mixed with two milliliters of quartz sand (inert diluent, 40-80 mesh) to maintain isothermal conditions, and then they were packed in the tubular reactor. Prior to the reaction, the calcined catalysts were reduced in syngas with the $H_2/CO/N_2$ of 1 : 1 : 1 at ambient pressure with a designed temperature-programmed procedure, which was employed as follows: RT (room temperature)→150 °C with a heating rate of 5 °C/min; 150 °C→300 °C with a heating rate of 3 °C/min; keeping at 300 °C for 2 h. After reduction, the reaction was conducted at a stationary state under reaction conditions of 3 MPa, 553-583 K, $V(H_2)/V(CO)/V(N_2)$=90/60/10 and CHSV=3,000 h^{-1}. The products were analyzed by two on-line GCs during the reaction. CH_4, N_2, CO, and CO_2 were analyzed by a TCD GC equipped with a TDX-01 column; hydrocarbons, alcohols were analyzed by an FID GC equipped with a TG-BONGQ column.

CO conversion rate was calculated as the mole percentage of carbon monoxide converted to products:

$$X_{CO}\,(\mathrm{mol\%}) = \frac{CO_{in} - CO_{out}}{CO_{in}} \times 100\% \tag{1}$$

The CO_2-free selectivity to a given product (S_i) was based on the total number of carbon atoms in the products except CO_2:

$$S_i = \frac{(n_i y_i)}{(\sum n_i y_i)} \times 100\% \tag{2}$$

where n_i($n_i \geq 1$) was the number of carbon atoms in component i, and y_i was the mole fraction of component i in the product stream.

Space time yield (STY) was calculated as weight of desired products (such as alcohols) produced per unit volume catalyst and per unit time:

$$\mathrm{STY}(\mathrm{g\,mL_{cat}^{-1}\,h^{-1}}) = \frac{\text{weight of alcohols produced (g)}}{\text{volume of catalyst (mL)} \times \mathrm{h}} \tag{3}$$

Anderson-Schulz-Flory (A-S-F) distribution describes the alcohol chain length distribution. That is, if the alcohol chain was formed step-wise by insertion or addition of C_1 intermediates with constant growth probability (α), then the chain length distribution was given by the A-S-F distribution [19]. The equation can be expressed as follows:

$$\frac{W_n}{n} = (1-\alpha)^2 a^{n-1} \rightarrow \ln\left(\frac{V_n}{n}\right) = n \ln\alpha + c \tag{4}$$

3. Catalyst Characterization

3-1. N_2 Adsorption-desorption

N_2 Adsorption and desorption isotherms were collected on an Autosorb-6 at 75 K. Prior to the measurements, the sample was degassed at 573 K until a stable vacuum of about 0.67 Pa was reached.

3-2. TPR

Prior to the experiment, the sample (50 mg) was purged with Ar at 100 °C in a flow rate of 30 mL/min for 2 h so that most of physically adsorbed H_2O could be removed from the samples. The TPR experiments were performed using a micro-fixed bed reactor connected with a thermal conducted detector (TCD). The temperature ramped from 50 °C to 400 °C with a ramping rate of 5 K/min in a 10% H_2/Ar flow (30 mL/min). The quantitative H_2 consumption was also evaluated for each sample.

3-3. XRD

XRD patterns were obtained with a Rigaku diffractometer (D/MAX 2550 VB/PC) using CuK_α radiation γ=0.1540589 nm (1.540589 Å).

3-4. XPS

XPS measurements were performed on an ESCALAB 250 (Thermo-VG Scientific, USA) spectrometer with AlK_α radiation. The C1s peak at a binding energy of 284.6 eV was generally fixed as a calibration standard for subtracting the surface charging effect.

RESULTS AND DISCUSSION

1. Catalyst Characterization

1-1. Textural and Structural Properties of Catalysts

The textural properties of the calcined catalysts are listed in Table

Table 1. The texture parameters of calcined catalysts

Catalyst	BET surface area [m^2g^{-1}]	Pore volume [cm^3g^{-1}]	Pore diameter [nm]
Cu/CeO_2	144	0.26	7.3
$CuNi/CeO_2$	155	0.23	5.8
$CuMo/CeO_2$	148	0.19	5.1
$CuNiMo/CeO_2$	158	0.16	4.1
$CuNiMoP/CeO_2$ (cop)	153	0.18	5.3
$CuNiMoP/CeO_2$ (imp)	150	0.17	4.4

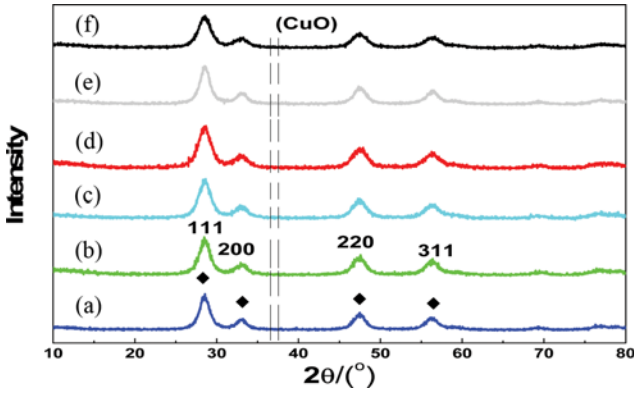

Fig. 1. XRD patterns of fresh catalysts (a) Cu/CeO_2, (b) $CuNi/CeO_2$, (c) $CuMo/CeO_2$, (d) $CuNiMo/CeO_2$, (e) $CuNiMoP/CeO_2$ (cop), (f) $CuNiMoP/CeO_2$ (imp), (◆) CeO_2.

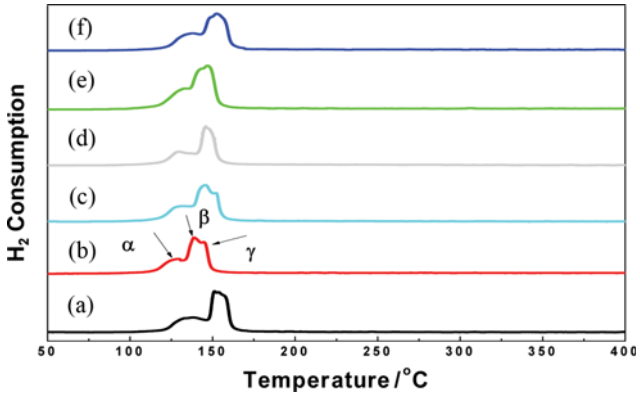

Fig. 3. H_2-TPR profiles of the catalysts (a) Cu/CeO_2, (b) $CuNi/CeO_2$, (c) $CuMo/CeO_2$ (d) $CuNiMo/CeO_2$, (e) $CuNiMoP/CeO_2$ (cop), (e) $CuNiMoP/CeO_2$ (imp).

1. Compared with Cu/CeO_2 catalyst, an increase in the BET surface area was observed over the other five catalysts. This evolution of the BET surface area was accompanied by a decrease in pore size of the catalyst. It may be concluded that promotion with Ni and Mo resulted in a small effect on the reducibility of Cu (the assumption was supported by the TPR results), which caused more Cu^{2+} ions doped in the CeO_2 positions. When this happened, the crystallization degree of the catalysts was decreased, which caused an increase of the BET surface area of the catalysts [20]. Catalysts promoted with Ni and Mo had higher CO conversion (in Table 3), which may be attributed to the increased BET surface area.

The XRD patterns of various fresh samples are shown in Fig. 1. As one can see, CeO_2 support showed four distinct reflections corresponding to the (1 1 1), (2 0 0), (2 2 0), and (3 1 1) crystallographic planes, indicating that the CeO_2 support had a fluorite structure with cubic cells. However, XRD peaks due to CuO were not detected in all samples with low CuO content. Xu et al. [21] found that the presence of Ce oxide species favored copper dispersion and formation of small Cu metal crystallites over Cu0.5Mg5CeO*x* catalyst. Luo et al. reported that weak diffraction peaks of CuO could be seen at a CuO content of 28.3 mol% [12]. The content of NiO, MoO_2 or $NiMoO_4$ might also be too low to be detected. In Fig. 2, the XRD diffraction patterns of reduced $CuNi/CeO_2$ catalyst were similar to those of fresh $CuNi/CeO_2$ catalyst, indicating that no changes happened in the crystal phase when catalyst was reduced.

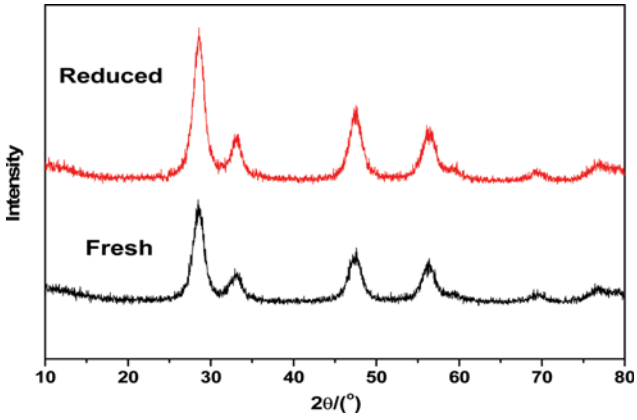

Fig. 2. XRD patterns of reduced and fresh $CuNi/CeO_2$ catalyst.

1-2. H_2-temperature-programmed Reduction

H_2-TPR profiles of the six catalysts are presented in Fig. 3. The profiles show that these peaks of catalysts A-E (F may be effected by the pyrogallol through impregnation) shifted to lower temperatures compared with those of Cu/CeO_2. This observation demonstrated that catalysts promoted with Ni and Mo resulted in a positive effect on the reducibility of Cu, which was consistent with the BET result. In addition, a reduction profile consisting of three peaks for copper-cerium catalysts was observed, generally named α-, β-, and γ-peak ordered by the increasing temperature [22,23]. Luo et al. [21] reported the presence of three different CuO species: highly dispersed CuO, Cu^{2+} in the CeO_2 lattice, and the bulk CuO species, respectively. Based on the above-mentioned, it was supposed that the first peak (α-peak) corresponds to the reduction of highly dispersed CuO and the second peak (β-peak) was associated with the reduction of Cu^{2+} in the CeO_2 lattice. The last peak (γ-peak) could be assigned to some extent of surface reduction of ceria by hydrogen split from the reduced copper moieties over its surface [24,25]. It was also observed that the $CuNi/CeO_2$ had a significant γ-peak, which might be attributed to the positive effect of Ni on hydrogen split.

1-3. XPS Analysis

Binding energy values from the XPS experiments are presented in Figs. 4 and 5, in which the parent peak was deconvoluted to four peaks. The binding energy was corrected for surface charging by taking the C1s peak of contaminant carbon as a reference at 284.8 eV. Fig. 4 and Fig. 5 show a weak satellite peak, which suggests that Cu^+ existed and no Cu^{2+} oxide existed in the $CuNiMo/CeO_2$ catalyst as well as $CuNiMoP/CeO_2$ (cop). However, whether Cu^0 existed or not was still unknown. Liu et al. reported that both Cu^0 and Cu^+ species were essential to the synthesis of methanol over Cu-based catalysts. Besides, the redox equilibrium ($Ce^{4+}+Cu \leftrightarrow Ce^{3+}+Cu^+$) could form between the CeO_2 support and Cu particles in the Cu/CeO_2 [15,26,27]. The differentiation of Cu^+ and Cu^0 species was achieved by combining with the Cu LMM Auger electron spectra in Fig. 6 [28]. Figs. 4 and 5 show kinetic energy of two peaks at about 916.2 eV [29] and 918.1 eV [30], which were due to

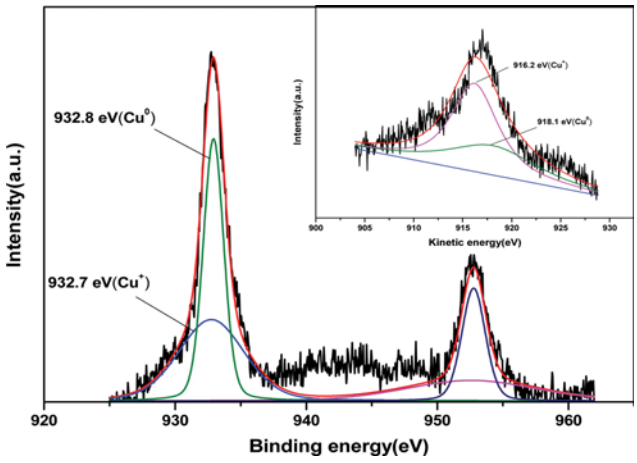

Fig. 4. XPS spectra of Cu2p region of reduced CuNiMo/CeO_2 catalyst.

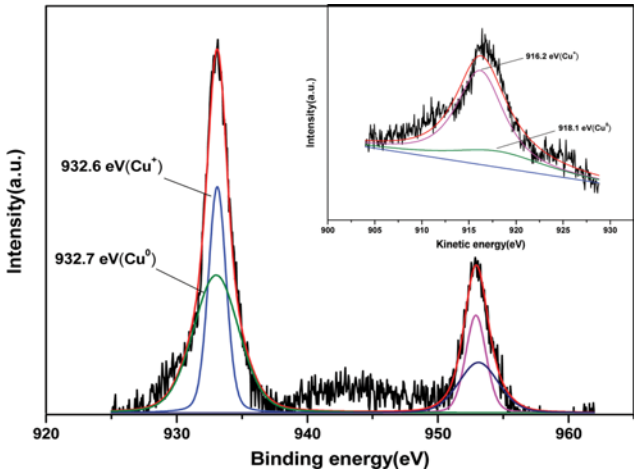

Fig. 5. XPS spectra of Cu2p region of reduced CuNiMoP/CeO_2 (cop) catalyst.

Cu^+ and Cu^0, respectively. Feng et al. suggested that the absorbed pyrogallol could form complexes with the cobalt and copper ions on the MWNTs when pyrogallol was used in preparing the catalyst [18]. In our study, CuNiMo/CeO_2 showed binding energy of two peaks at 932.8 eV (Cu^0) [21,31,32] and 932.7 eV (Cu^+) [33,34]. When pyrogallol was used in preparing the catalyst, the two peaks shifted to the lower binding energy slightly, at 932.7 eV (Cu^0) [35, 36] and 932.6 eV (Cu^+) [37,38] respectively, which was more obvious in the Cu LMM Auger electron spectra (in Fig. 4 and 5). Furthermore, it was noted that CuNiMo/CeO_2 and CuNiMoP/CeO_2 (cop) catalysts enjoyed a Cu^+/Cu^0 ratio at 1.05 and 0.64, respectively. That is, CuNiMo/CeO_2 catalyst had a higher Cu^+/Cu^0 ratio than CuNiMoP/CeO_2 (cop) in Table 2. According to Fujitani et al. [39], the support effect or doping metal oxides into copper catalysts on methanol synthesis reaction was ascribed to the ratio of Cu^+ to Cu^0 on the surface of copper particles. And the amount of surface Cu^+ was responsible for methanol production rate as Cu^+ sites were essential for CO adsorption [40]. In the meantime, the methanol selectivity was significantly decreased when pyrogallol was used in preparing the catalyst. Based on the above-mentioned, we came to the conclusion that pyrogallol could form complexes with Cu^+ on the CeO_2 support (White et al. used polarography to provide evidence concerning the formation of metal ion-pyrogallol complexes [41]. Safavi et al. determined the trace amounts of copper based on the accumulation of copper-pyrogallol complex [42]), which might be the mechanism about pyrogallol used in preparing the Cu-base catalyst.

Table 2. Comparison of XPS results between CuNiMo/CeO_2 and CuNiMoP/CeO_2 (cop) catalysts

Catalyst	Cu^0 position (eV)	Cu^+ position (eV)	Cu^+/Cu^0
CuNiMo/CeO_2	932.8	932.7	1.05
CuNiMoP/CeO_2 (cop)	932.7	932.6	0.64

2. Catalyst Performance

2-1. Effect of Metal Promotion on the Performance of Cu/CeO_2 Catalyst

The performance of the Ni-promoted, Mo-promoted and NiMo-promoted Cu/CeO_2 catalyst in the higher alcohols synthesis is shown in Table 3. When promoted with metal Ni, Cu/CeO_2 catalyst employed higher CO conversion, STY_{C-OH} and STY_{C2+OH}, while alcohol selectivity decreased (mainly caused by methanol), which coincided with the study of Li et al. [43]. In their study, Ni was effective in enhancing the activity and $C^{2+}OH$ selectivity for higher alcohol synthesis over Ni/K_2CO_3/MoS_2 catalyst. For CuMo/CeO_2 catalyst, it had a higher CO conversion and S_{C2+OH}/S_{MeOH} (especially for higher ethanol and propanol selectivity), though alcohol selectivity decreased significantly compared with Cu/CeO_2 catalyst.

Note that Cu/CeO_2 catalyst employed higher CO conversion when promoted with Ni and Mo simultaneously, as well as STY_{C2+OH} (in Table 3). It might be suggested that the existence of the interaction between Ni and Mo was beneficial for catalytic activity and higher alcohols synthesis. Liakakou et al. [17] found that the monometallic Ni and Mo AC-supported catalysts, which were both inactive in CO hydrogenation under reaction conditions, got a high catalytic performance when they were simultaneously used in preparing the catalyst. It was demonstrated that the Ni-Mo synergistic effect was essential for the activation of CO over K-promoted NiMo catalyst supported on activated carbon. Meanwhile, the Ni-Mo synergistic effect and the formation of Ni-O-Mo functionalities were mandatory in order to produce a fair amount of oxygenates. In this study, the existence of active site Cu and metal Ni and Mo served as promoters might be the reason why no fairly obvious result was obtained.

2-2. Effect of Pyrogallol over CuNiMo/CeO_2 Catalyst

Few works about pyrogallol applied in the synthesis of higher alcohols have been reported. Feng et al. [18] found that pyrogallol made CO conversion increase and the methanol selectivity decrease significantly for higher alcohols synthesis over CNT-SG catalyst. In this study, two methods were employed to prepare CuNiMoP/CeO_2 catalyst, coprecipitation and impregnation respectively. Table 3 shows that there was no big difference between these two catalysts' performance made by different methods. In Fig. 6, compared with CuNiMo/CeO_2 catalyst, the CuNiMoP/CeO_2 (cop) catalyst had a significant

Table 3. Catalytic performance over various catalysts for the synthesis of higher alcohol at reaction condition: n(H_2)/n(CO)=1.5; T=300 °C; P=3 MPa; GHSV=3,000 h^{-1}

Catalyst	X_{CO}	S_{alc}	STY_{alc} ($gmL_{cat}^{-1}h^{-1}$)	$STY_{C^{2+}OH}$ ($gmL_{cat}^{-1}h^{-1}$)	$S_{C^{2+}OH}/S_{MeOH}$
Cu/CeO_2	22.96	89.80	0.28	0.047	0.23
$CuNi/CeO_2$	26.86	84.52	0.31	0.053	0.24
$CuMo/CeO_2$	27.60	62.83	0.22	0.048	0.31
$CuNiMo/CeO_2$	31.35	71.30	0.32	0.060	0.27
$CuNiMoP/CeO_2$ (cop)	32.85	64.29	0.30	0.065	0.35
$CuNiMoP/CeO_2$ (imp)	30.38	61.14	0.25	0.060	0.37

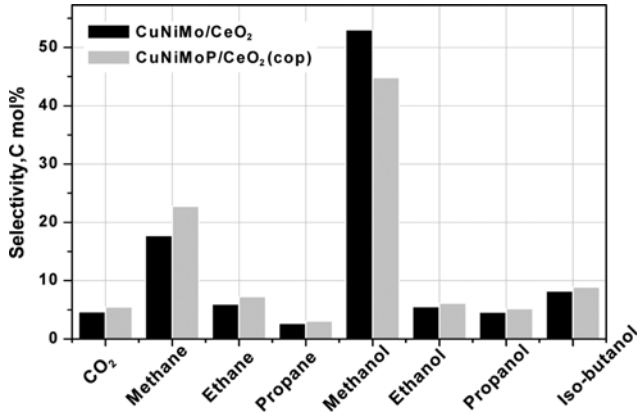

Fig. 6. Products selectivity over $CuNiMo/CeO_2$ and $CuNiMoP/CeO_2$ (cop) catalysts at reaction condition: n(H_2)/n(CO)=1.5; T=300 °C; P=3 MPa; GHSV=3,000 h^{-1}.

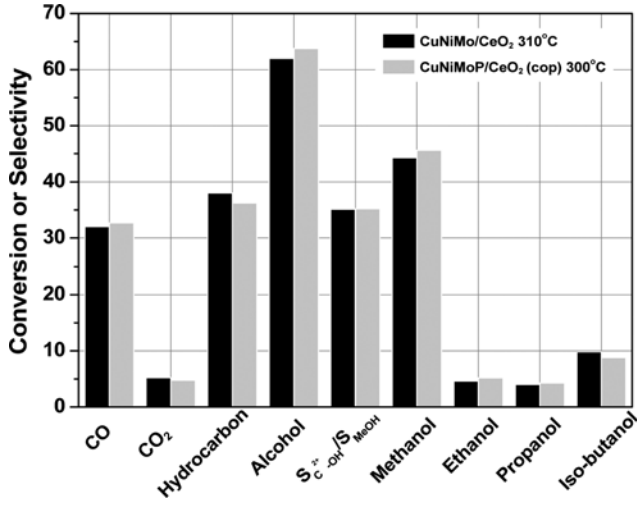

Fig. 7. Comparison of production selectivity over $CuNiMo/CeO_2$ catalyst at 300 °C and $CuNiMoP/CeO_2$ (cop) catalyst at 310 °C (n(H_2)/n(CO)=1.5; P=3 MPa; GHSV=3,000 h^{-1}).

increase in methane selectivity and a significant decrease in methanol selectivity. Furthermore, the ethanol, propanol and isobutanol selectivity had a slight increase, as well as CO conversion and hydrocarbon selectivity. The methanol selectivity was decreased from 52.99% to 44.81% and the S_{C2+OH}/S_{MeOH} ratio increased from 0.27 to 0.35 when pytogallol was used in preparing the catalyst. That is, pyrogallol could exert a positive effect on improving the C^{2+}-OH selectivity.

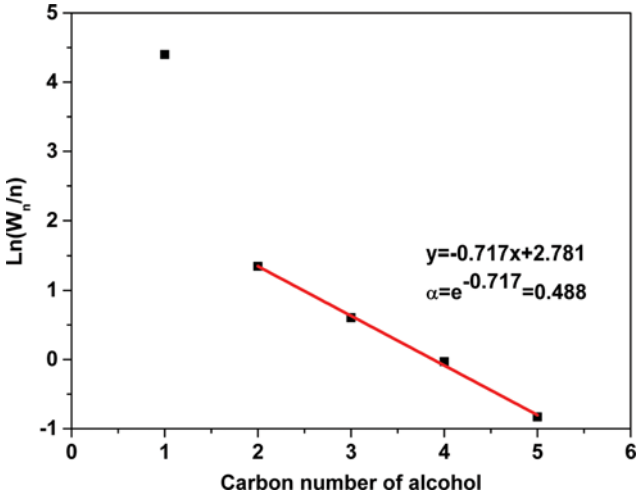

Fig. 8. ASF plot for the distribution of alcohols over $CuNiMo/CeO_2$ catalyst at reaction condition: n(H_2)/n(CO)=1.5; T=300 °C; P=3 MPa; GHSV=3,000 h^{-1}.

Also, $CuNiMoP/CeO_2$ catalyst performed at 300 °C had almost the same product distribution as $CuNiMo/CeO_2$ catalyst performed at 310 °C in Fig. 7. This may be explained by the effect of reaction temperature. When reaction temperature increased from 300 °C to 310 °C, the selectivity of methane would increase and the selectivity of methanol would decrease over $CuNiMo/CeO_2$ catalyst. In addition, the C^{2+}-OH selectivity became slightly higher, as well as the CO conversion. Therefore, the effect of pyrogallol on higher alcohol synthesis was similar to the effect of reaction temperature in some term. Besides, higher alcohols synthesis was usually favorable only in a narrow range of temperatures, 280-310 °C [44]. That is, pyrogallol used in preparing the $CuNiMo/CeO_2$ catalyst could serve as a "temperature addictive agent," which may be beneficial for decreasing the power that catalytic reaction needed. It required further investigation whether there existed a familiar effect on another catalytic system when using pyrogallol in preparing the catalysts.

Fig. 8 and Fig. 9 show the A-S-F plot for the distribution of alcohols over $CuNiMo/CeO_2$, $CuNiMoP/CeO_2$ (cop) and $CuNiMoP/CeO_2$ (imp) at 300 °C. The amount of methanol was very large and the point of methanol was not on the straight line of higher alcohols. Because the points of higher alcohols were on one straight line in the A-S-F plot, the chain growth probability could be calculated using the slope of the imitation straight line of the higher alco-

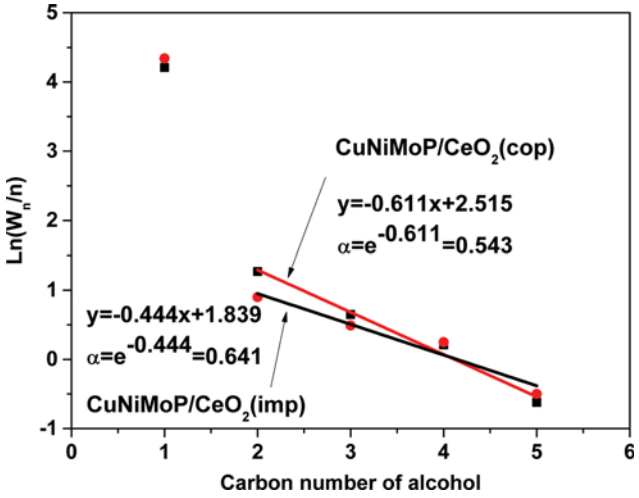

Fig. 9. ASF plot for the distribution of alcohols over CuNiMoP/CeO_2 (cop) and CuNiMoP/CeO_2 (imp) catalyst at reaction condition: n(H_2)/n(CO)=1.5; T=300 °C; P=3 MPa; GHSV=3,000 h^{-1}.

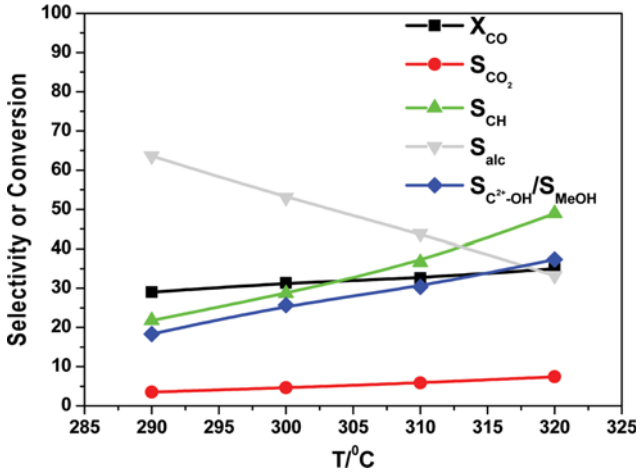

Fig. 11. The effect of reaction temperature in the synthesis of higher alcohols over CuNiMo/CeO_2 (n(H_2)/n(CO)=1.5; P=3 MPa; GHSV=3,000 h^{-1}).

hols. Compared with CuNiMo/CeO_2 catalyst in Fig. 8, which was calculated as 0.488, CuNiMoP/CeO_2 (cop) and CuNiMoP/CeO_2 (imp) got higher chain growth probabilities, which were calculated as 0.543 and 0.641, respectively. In other words, it was favorable for chain growth of higher alcohols when pyrogallol was used in preparing the CuNiMo/CeO_2 catalyst, especially for impregnation method.

A series of experiments with different amounts of pyrogallol was further carried out, varying from molar ratio of 1 : 0.1(Cu : P) to 1 : 0.5. In Fig. 10, it was noticed that the methanol selectivity decreased and the S_{C2+OH}/S_{MeOH} ratio increased with the increasing amount of pyrogallol. Besides, the conversion of CO had a slightly increase.

2-3. Effect of Reaction Temperature over CuNiMo/CeO_2 Catalyst

Fig. 11 shows that the CO conversion increased at a slow speed from 29.05% to 33.02%, when the reaction temperature increased from 290 to 320 °C. However, the selectivity for hydrocarbon increased from 21.78% to 36.58% and then the selectivity for alcohol decreased from 78.22% to 63.42% with the increasing reaction temperature. On the other hand, the synthesis of alcohols is an exothermic reaction and is thermodynamically limited by high temperature [15], the S_{C2+OH}/S_{MeOH} ratio increased from 18.32% to 37.34% with increasing temperature due to the increased C^{2+}-OH selectivity and decreased methanol selectivity.

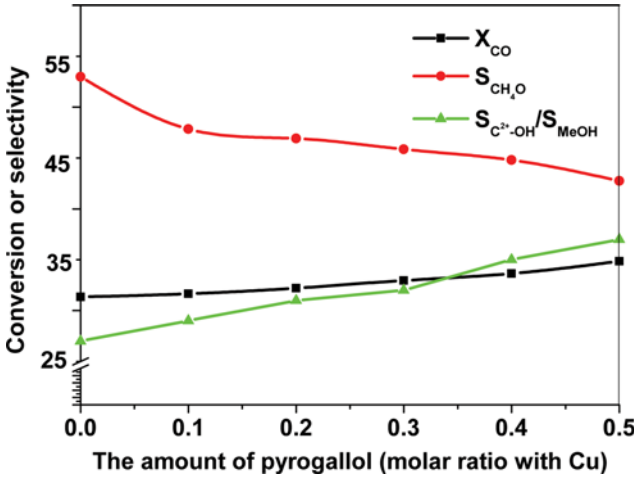

Fig. 10. The effect of pyrogallol in the synthesis of higher alcohols over CuNiMo/CeO_2 (n(H_2)/n(CO)=1.5; P=3 MPa; T=300 °C; GHSV=3,000 h^{-1}).

CONCLUSION

Cu/CeO_2 catalyst modified with Ni and Mo achieved high activity and high selectivity for higher alcohols under mild reaction conditions (T=300 °C; P=3 MPa; GHSV=3,000 h^{-1}; (n(H_2)/n(CO)= 1.5). Compared with Cu/CeO_2, CuNiMo/CeO_2 catalyst shared a large BET surface area and a lower TPR reduced temperature, which suggested that Ni and Mo could promote the reducibility of Cu and then get a higher catalytic activity. Cu/CeO_2 catalyst employed a much higher CO conversion when promoted with Ni and Mo simultaneously, as well as STY_{C2+OH}, which may demonstrate that the interaction between Ni and Mo is also needed for catalytic activity and higher alcohols synthesis.

The pyrogallol used in preparing the CuNiMo/CeO_2 catalyst could exert a positive effect on improving the C^{2+}-OH selectivity. It could also increase the CO conversion slightly. Pyrogallol also had a significant effect on decreasing methanol selectivity, due to the formation of complexes with Cu^+ on the CeO_2 support, which was supported by XPS results. On the other hand, pyrogallol could serve as a "temperature addictive agent," which may be used to save power for catalyst reaction for higher alcohols synthesis.

REFERENCES

1. J. Bao, J. He, Y. Zhang, Y. Yoneyama and N. Tsubaki, *Angew. Chem. Int. Ed.*, **47**, 353 (2008).

2. J. J. Spivey and A. Egbebia, *Chem. Soc. Rev.*, **36**, 1514 (2007).
3. Q. Zhang, J. Kang and Y. Wang, *ChemCatChem.*, **2**, 1030 (2010).
4. R. G. Herman, *Catal. Today*, **55**, 233 (2000).
5. P. Courty, P. Chaumette, C. Raimbault and P. Travers, *Rev. Inst. Fr. Pet.*, **45**, 561 (1990).
6. J. J. Spivey and A. Egbebi, *Chem. Soc. Rev.*, **36**, 1514 (2007).
7. J. M. Christensen, P. M. Mortensen, R. Trane, P. A. Jensen and A. D. Jensen, *Appl. Catal. A: Gen.*, **366**, 29 (2009).
8. D. H. Mei, R. Rousseau, S. M. Kathmann, V. A. Glezakou, M. H. Engelhard, W. L. Jiang, C. M. Wang, M. A. Gerber, J. F. White and D. J. Stevens, *J. Catal.*, **271**, 325 (2010).
9. Q. W. Zhang, X. H. Li and K. Fujimoto, *Appl. Catal. A: Gen.*, **309**, 28 (2006).
10. M. B. Jorge, G.-C. Anne and Y. K. Andrei, *Chemcatchem*, **6**, 1788 (2014).
11. R. Xu, S. Zhang and C. B. Roberts, *Ind. Eng. Chem. Res.*, **52**, 14514 (2013).
12. M. Xu, M. J. L. Gines, A.-M. Hilmen, B. L. Stephens and E. Iglesia, *J. Catal.*, **171**, 130 (1997).
13. A.-M. Hilmen, M. Xu, M. J.L. Gines and E. Iglesia, *Appl. Catal. A: Gen.*, **169**, 355 (1998).
14. D. S. Kim, I. E. Wachs and K. Segawa, *J. Catal.*, **149**, 268 (1994).
15. Y. Liu, K. Murata, M. I. Takahara and K. Okabe, *Fuel*, **104**, 62 (2010).
16. M. Xiang, D. Li, H. Xiao, J. Zhang, H. Qi, W. Li, B. Zhong and Y. Sun, *Fuel*, **87**, 599 (2008).
17. E. T. Liakakou, E. Heracleous, K. S. Triantafyllidis and A. A. Lemonidou, *Appl. Catal. B*, **165**, 296 (2015).
18. W. Feng, Q. Wang, B. Jiang and P. Ji, *Ind. Eng. Chem. Res.*, **50**, 11067 (2011).
19. A. Tavakoli, M. Sohrabi and A. Kargari, *J. Chem. Eng.*, **136**, 358 (2008).
20. Y. Liu, T. Hayakawa, T. Ishii, M. Kumagai, H. Yasuda, K. Suzuki, S. Hamakawa and K. Murata, *Appl. Catal. A: Gen.*, **210**, 301 (2001).
21. M.-F. Luo, J.-M. Ma, J.-Q. Lu, Y.-P. Song and Y.-J. Wang, *J. Catal.*, **246**, 52 (2007).
22. G. Avgouropoulos, T. Ioannides and H. Matralis, *Appl. Catal. B: Environ.*, **56**, 87 (2005).
23. X. Zheng, X. Zhang, X. Wang, S. Wang and S. Wu, *Appl. Catal. A: Gen.*, **295**, 142 (2005).
24. M. Manzoli, R. di Monte, F. Boccuzzi, S. Coluccia and J. Kaspar, *Appl. Catal. B: Environ.*, **61**, 192 (2005).
25. F. Mariño, B. Schönbrod, M. Moreno, M. Jobbágy, G. Baronetti and M. Laborde, *Catal. Today*, **133-135**, 735 (2008).
26. Y. Liu, T. Hayakawa, K. Suzuki, S. Hamakawa, T. Tsunoda, T. Ishii and M. Kumagai, *Appl. Catal. A: Gen.*, **223**, 137 (2002).
27. Y. Liu, T. Hayakawa, T. Tsunoda, K. Suzuki, S. Hamakawa, K. Murata, R. Shiozaki, T. Ishii and M. Kumagai, *Top Catal.*, **22**, 205 (2003).
28. S. Velu, K. Suzuki and C. S. Gopinath, *J. Phys. Chem. B*, **106**, 12737 (2002).
29. F. M. Capece, V. Dicastro, C. Furlani, G. Mattogno, C. Fragale, M. Gargano and M. Rossi, *J. Electron Spectrosc. Relat. Phenom.*, **27**, 119 (1982).
30. J. Haber, T. Machej, L. Ungier and J. Ziolkowski, *J. Solid State Chem.*, **25**, 207 (1978).
31. F. M. Capece, V. Dicastro, C. Furlani, G. Mattogno, C. Fragale, M. Gargano and M. Rossi *J. Electron Spectrosc. Relat. Phenom.*, **27**, 119 (1982).
32. J. Hedman, M. Klasson, R. Nilsson, C. Nordling, M. F. Sorokina, O. I. Kljushnikov, S. A. Nemnonov, V. A. Trapeznikov and V. G. Zyranov, *Phys. Scripta*, **4**, 195 (1971).
33. G. Johansson, J. Hedman, A. Berndtsson, M. Klasson and R. Nilsson, *J. Electron Spectrosc. Relat. Phenom.*, **2**, 295 (1973).
34. D. Chadwick and T. Hashemi, *Corros. Sci.*, **18**, 39 (1978).
33. J. G. Jolley, G. G. Geesey, M. R. Haukins, R. B. Write and P. L. Wichlacz, *Appl. Surf. Sci.*, **37**, 469 (1989).
35. C. Battistoni, G. Mattongno, E. Paparazzo and L. Naldini, *Inorg. Chim. Acta*, **102**, 1 (1985).
36. C. J. Powell, N. E. Erickson and T. Jach, *J. Vac. Sci. Technol.*, **20**, 625 (1981).
37. J. Haber, T. Machej, L. Ungier and J. Ziolkowski, *J. Solid State Chem.*, **25**, 207 (1978).
38. N. S. McIntyre, S. Sunder, D. W. Shoesmith and F. W. Stanchell, *J. Vac. Sci. Technol.*, **18**, 714 (1981).
39. T. Fujitani, M. Satio, Y. Kanai, T. Kakumoto, T. Watanabe, J. Nakamura and T. Uchijima, *Catal. Lett.*, **25**, 271 (1994).
40. Q. Yan, P. T. Doan, T. Hossein, C. G. Amit and G. W. Mark, *J. Phys. Chem. C*, **112**, 11847 (2008).
41. S. M. Cletus White and A. J. Bard, *Anal. Chem.*, **38**, 61 (1966).
42. A. Safavi and E. Shams, *Anal. Chim. Acta*, **385**, 265 (1999).
43. D. Li, C. Yang, H. Qi, H. Zhang, W. Li, Y. Sun and B. Zhong, *Catal. Commun.*, **5**, 605 (2004).
44. M. Gupta, M. L. Smith and J. J. Spivey, *ACS Catal.*, **1**, 641 (2011).